Current Research in Pharmacology and Drug Discovery 4 (2023) 100142

Contents lists available at ScienceDirect

Current Research in Pharmacology and Drug Discovery

journal homepage: www.journals.elsevier.com/current-research-in-pharmacology-and-drug-discovery

Characterization of a novel positive allosteric modulator of the α_{1A}-Adrenergic receptor

Robert S. Papay [a], Jonathan D. Macdonald [b], Shaun R. Stauffer [b], Dianne M. Perez [a,*]

[a] The Department of Cardiovascular & Metabolic Sciences, Lerner Research Institute, The Cleveland Clinic Foundation, 9500 Euclid Ave, Cleveland, OH, 44195, USA
[b] Center for Therapeutics Discovery, Lerner Research Institute, The Cleveland Clinic Foundation, 9500 Euclid Ave, Cleveland, OH, 44195, USA

ARTICLE INFO

Keywords:
Positive allosteric modulator
alpha1-adrenergic receptor
Norepinephrine

ABSTRACT

α_1-Adrenergic Receptors (ARs) are G-protein Coupled Receptors (GPCRs) that regulate the sympathetic nervous system via the binding and activation of norepinephrine (NE) and epinephrine (Epi). α_1-ARs control various aspects of neurotransmission, cognition, cardiovascular functions as well as other organ systems. However, therapeutic drug development for these receptors, particularly agonists, has been stagnant due to unwanted effects on blood pressure regulation. We report the synthesis and characterization of the first positive allosteric modulator (PAM) for the α_1-AR based upon the derivation of the α_{1A}-AR selective imidazoline agonist, cirazoline. Compound 3 (Cmpd-3) binds the α_{1A}-AR with high and low affinity sites (0.13pM; 54 nM) typical of GPCR agonists, and reverts to a single low affinity site of 100 nM upon the addition of GTP. Comparison of Cmpd-3 versus other orthosteric α_{1A}-AR-selective imidazoline ligands reveal unique properties that are consistent with a type I PAM. Cmpd-3 is both conformationally and ligand-selective for the α_{1A}-AR subtype. In competition binding studies, Cmpd-3 potentiates NE-binding at the α_{1A}-AR only on the high affinity state of NE with no effect on the Epi-bound α_{1A}-AR. Moreover, Cmpd-3 demonstrates signaling-bias and potentiates the NE-mediated cAMP response of the α_{1A}-AR at nM concentrations with no effects on the NE-mediated inositol phosphate response. There are no effects of Cmpd-3 on the signaling at the α_{1B}- or α_{1D}-AR subtypes. Cmpd-3 displays characteristics of a pure PAM with no intrinsic agonist properties. Specific derivation of Cmpd-3 at the R1 *ortho*-position recapitulated PAM characteristics. Our results characterize the first PAM for the α_1-AR and holds promise for a first-in-class therapeutic to treat various diseases without the side effect of increasing blood pressure intrinsic to classical orthosteric agonists.

1. Introduction

A large number of pharmaceuticals are designed to target G-protein Coupled Receptors (GPCRs) because of their cell surface availability, low molecular weight, signal amplification properties, and well-defined biological activities. Most current pharmaceuticals bind to the orthosteric site, defined as the binding site for the endogenous agonist(s), such as norepinephrine (NE) or epinephrine (Epi) for the adrenergic receptor (AR) family. The orthosteric site is typically highly conserved in the amino acids forming the binding pocket between GPCR family members. However, the large number of subtypes in a GPCR family and common pathways in binding and activation allows for potential adverse side effects of ligands by also targeting other closely-related receptor subtypes and off-target sites.

A newer class of drugs called allosteric modulators are rapidly being developed to enhance specificity with reduced side effects by binding to noncompetitive unique sites on the receptor distinct from the orthosteric site (Christopoulos and Kenakin, 2002). Allosteric modulators commonly alter the characteristics of drug-bound receptor binding and signaling. Allosteric modulators are categorized as negative allosteric (NAM), positive allosteric (PAM) or silent/neutral (SAM) allosteric modulators. PAMs enhance while NAMs inhibit ligand activity through either efficacy and/or potency but only when an orthosteric ligand is bound to the receptor at the same time (Christopoulos, 2014). Therefore, an "off" receptor stays inactive when the orthosteric ligand is absent even if the PAM/NAM is circulating in the body, a property that would potentially diminish side effects.

For GPCRs, a large number of allosteric modulators have already been described and developed and is highly represented by the class A GPCR superfamily with many in clinical trials (Wold et al., 2019). The α_{1A}-AR subtype is a class A GPCR together with two-other closely related subtypes (α_{1B}, α_{1D}) plus six other more distantly-related subtypes (β_1, β_2, β_3,

* Corresponding author. NB50, 9500 Euclid Ave, The Cleveland Clinic Foundation, Cleveland, OH, 44195, USA.
E-mail address: perezd@ccf.org (D.M. Perez).

https://doi.org/10.1016/j.crphar.2022.100142
Received 8 August 2022; Received in revised form 27 October 2022; Accepted 15 November 2022

α_{2A}, α_{2B}, α_{2C}). PAMs and NAMs have been previously described for the β-AR (Ahn et al., 2017, 2018). In contrast, only NAMs but no PAMs have been described for the α_1-and α_2-ARs (Leppik et al., 2000; Leppik and Birdsall, 2000; Sharpe et al., 2003; Campbell et al., 2017).

We have previously shown *in vivo* and *in vitro* that the α_{1A}-AR subtype is expressed in key cognitive centers of the brain, is both cardiac and neuroprotective, and activation of this receptor can increase lifespan, treat heart failure, increase cognition, synaptic plasticity, long term potentiation, and adult neurogenesis in normal WT mice (Rorabaugh et al., 2005; Papay et al., 2006; Gupta et al., 2009; Doze et al., 2011; Collette et al., 2014; Shi et al., 2016; Perez, 2020, 2021a). Our initial goal was to design highly-selective novel α_{1A}-AR brain-penetrant partial agonists using the imidazoline backbone of the mildly-selective α_{1A}-AR agonist cirazoline to use in preclinical studies. Previous studies have suggested that imidazoline-based agonists such as cirazoline demonstrate greater selectivity for the α_{1A}-AR over α_{1B}- or α_{1D}- ARs, or α_2-ARs (Minneman et al., 1994; Whitlock et al., 2008) and with weaker effects on blood pressure than phenethylamine-based agonists (Blue et al., 2004; Musselman et al., 2004; Bishop, 2007), reducing unwanted cardiovascular side effects of α_1-AR agonists. We postulated that the weaker blood pressure effects of α_{1A}-AR selective imidazolines was due to their ability to bias-signaling towards cAMP when compared to phenethylamine-type agonists (Evans et al., 2011; da Silva Junior et al., 2017) which are more strongly coupled to inositol phosphate (IP) signaling. IP signals activate calcium release and the contraction of vascular smooth muscle (Kiowski, 1990; Kiowski et al., 1989; O-Uchi et al., 2008; Ottolini et al., 2019). One of our compounds, cmpd-3, and related derivations described herein, has resulted in the development of the first described PAMs for the α_{1A}-AR receptor through a unique ligand-bias and signaling selectivity that is expected to enhance therapeutic utility.

2. Materials and methods

Compound synthesis. Synthetic schemes and details of the target compound synthesis are reported in the Supplemental Information (S1). Cirazoline HCl (>99% purity) was purchased from Tocris (Avonmouth, Bristol, UK) and RO115-1240 HCl (Dabuzalgron, >98% purity) was purchased from The BioTek (Segundo, Ca). All compounds were confirmed for structure and purity (>98%) by HPLC, ^{1}H-NMR, and Mass Spectrometry (MS).

Radioligand Binding studies. Assays were performed in duplicate in HEM buffer, in a total assay volume of 1000 μl. Radioligand binding assays are composed of 5–10 μg of membranes as previously described (Perez et al., 1991), harvested from Rat −1 fibroblast cells stably-expressing α_1-AR subtypes. Binding studies were performed in HEM buffer composed of 20 mM HEPES, pH 7.4, 1.4 mM EGTA, 12.5 mM $MgCl_2$, pH to 7.4) and supplemented with 0.018% ascorbic acid, 0.005% BSA, 10 μM propranolol, and 0.1 μM rauwolscine and was preincubated first with membranes containing ARs for 4 h at 25 °C to achieve equilibrium conditions. The radioligand was then added, either 100–600 pM ^{125}I-(2-{[β-(4-Hydroxyphenyl) ethyl]aminomethyl}-1-tetralone hydrochloride) (HEAT) or ^{3}H-Norepinephrine (42 nM) and incubated with various doses of unlabeled compound or ligand with shaking at 25 °C for an additional hour. To convert all the conformations to a single low-affinity site in certain experiments, 0.5 mMGTP is added to the binding buffer. Binding data is analyzed using Graphpad Prism.

cAMP assay. Rat-1 fibroblasts expressing a single α_1-AR subtype are washed and re-plated into 24-well plates in Dulbecco's Modified Eagle Medium (DMEM) media without serum at approximately 2.4 x 10^4 cells/well. Cells are allowed to rest till the next day in a CO_2 incubator at 37 °C. The cells are washed twice with DMEM (no serum), then 1 ml of DMEM is added to each well. Cells are pre-incubated for 2 h at 37 °C in a CO_2 incubator with 10 μM propranolol, 0.1 μM rauwolscine, and the test compound, followed by 100–200 μM of 3-isobutyl-1-methylxanthine (IBMX) and either NE or Epi for an additional 2 h at 37 °C in a CO_2 incubator. NE or Epi are added either in a dose response (1 dose per well) or at a fixed concentration (PAM assay; 10^{-4} M) in addition to the test compound at either one or multiple concentrations. The reaction is concluded by aspirating the media and adding 0.1M HCl. The mixture is incubated for 20 min at room temperature. The cells are scraped and suspended until homogenous. The mixture is centrifuged at 1000 g for 10 min and the supernatant assayed the same day according to a manufacturer's cAMP kit (Cayman Select Cyclic AMP EIA kit #501040).

Total inositol phosphate assay. Cells expressing a single α_1-AR subtypes are washed and re-plated into 6-well plates containing DMEM media at approximately 5 x 10^4 cells/well. Cells are allowed to rest till the next day in a CO_2 incubator at 37 °C. Two μl of ^{3}H-inositol (at 1 μCi/mL, PerkinElmer NET 114 005 MC) is added to each well and incubated overnight in a CO_2 incubator at 37 °C. The cells are washed twice with DMEM (no serum), then 2 ml of DMEM (no serum) is added to each well. LiCl (10 mM, final) is added to each well and incubated for 1 h in a CO_2 incubator at 37 °C. NE or Epi are added either in a dose response (1 dose per well) in addition to the test compound at either one or multiple concentrations. The cells are further incubated for 1 h at 37 °C in a CO_2 incubator. The cells are assayed for total inositol phosphates (IP) as previously described using anion-exchange chromatography (Perez et al., 1993).

p-CREB activity. Rat-1 fibroblasts expressing the α_{1A}-AR were plated into 6-well dishes at a concentration of 2.8 x 10^6 cells and placed in a 37 °C/5% CO_2 incubator overnight. The following day the cells were washed twice with DMEM (no serum or additives). DMEM was added and the cells incubated for 1 h in the incubator. Propranolol (10 μM final, Sigma P-0884) and rauwolscine (0.1 μM final, Tocris 0891) were added to all wells and test wells also received Compd-3 (10^{-8} M, final) and incubated for an additional 2 h. NE (10^{-4} M final, Sigma A9512) was added to each well followed by IBMX (500 μM, Sigma I-5879) and incubated for 45 min, then washed once with 2 ml PBS. To assessed p-CREB, cells were lysed with 0.3 ml cold lysis buffer consisting of M-PER mammalian protein extraction reagent (Pierce #78501) containing 1X Halt protease & phosphatase inhibitor mix (Pierce #78441), 1X Protease Inhibitor Cocktail set III (Calbiochem 539134), 10 mM β-glycerophosphate, 10 mM sodium fluoride, 1 mM sodium vanadate, and 2 mM sodium pyrophosphate. The cells were scraped on ice and transferred to microfuge tubes. Tubes were centrifuged at 18,000 RCF at 4 °C for 20 min. The supernatant was transferred into new microcentrifuge tubes, an aliquot taken for protein quantitation (Pierce Micro BCA Protein Assay Kit #23235), and the samples stored at −20 °C.

100 μg lysate was boiled in a total of 40 μl sample buffer for 5 min containing 100 mM dithiothreitol (Sigma D9163) in 62.5 mM Tris, pH 6.7, 2% SDS, 10% glycerol and 0.04% bromophenol blue, followed by SDS-PAGE using a 10% Tris HCl gel (Biorad Mini-PROTEAN TGX gel #4561034). The gel was transferred using BioTrace pure nitrocellulose (Pall 66485) in Tris glycine buffer without SDS but containing 20% methanol. The nitrocellulose was blocked with 5% BSA in PBST for 1 h at room temperature, washed 3 × 5 min with PBST, and then incubated overnight at 4° with rabbit phospho-CREB antibody (pSer133, Cell Signaling #9198) at 1:1000 in 5% BSA in PBST. The membrane was washed 3 × 5 min before incubating with 1:10,000 goat anti-rabbit IgG HRP in 5% BSA in PBST for 1 h at room temperature. After washing 5 × 5 min, the membrane was incubated with 5 ml of each component of the HyGlo Chemiluminescent HRP Antibody Detection Reagent (Denville). After quantification, the blots were stripped and incubated with rabbit GAPDH (Cell Signaling, #2118) at 1:1000 dilution. The bands were quantified using the Image Studio Digits Version 4.0 program associated with the Li-Cor digital scanner model C-DIGit, normalized to GAPDH levels, and graphed using Prism software. P-CREB is identified at 43 kDa, and a phosphorylated form of the CREB-related protein ATF-1 also cross reacts (29 kDa, Cell Signalling #9191).

Statistics. Statistical testing was performed using an ANOVA and the Turkey's or Bonferroni's post hoc multiple comparison test to determine significant differences or a student's t-test. Significance was determined at $p < 0.05$.

3. Results

Cmpd-3 design and synthesis. Cmpd-3 was designed based upon the structure of cirazoline, an α_{1A}-AR agonist with 10-50-fold selectivity against the α_{1B}- and α_{1D}-AR subtypes (Hwa et al., 1995). This structure was chosen for derivatization because of its ability to bias cAMP signaling (Evans et al., 2011; da Silva Junior et al., 2017). We previously identified a number of residues in the α_{1A}-AR agonist binding pocket and the type of modifications needed in α_{1A}-AR ligands to increase selectivity (Hwa et al., 1995, 1996, 1996, 1996; Waugh et al., 2000, 2001; McCune et al., 2004; Perez, 2007). In particular are the aliphatic hydrophobic groups at the R1 *ortho*-position on the aromatic ring and the *N*- and *S*- substituents of sulfonamide at the R2 position (as denoted in Fig. 1). Because of our desire to design only partial agonists which would also lead to a weaker blood pressure effect, the R2 position contained a methyl-sulfonamide. One of the initial compounds we synthesized (Cmpd-3) displayed selective binding towards the α_{1A}-AR and was further characterized.

Cmpd-3 demonstrates α_{1A}-AR binding selectivity. We first determined equilibrium conditions of Cmpd-3 (10^{-5} M) in its competitive binding of ^{125}I-HEAT (data not shown) at the α_{1A}-AR. This was determined to be 1 h. As allosteric interaction can alter binding kinetics, further binding incubations were performed for 4 h to be sure equilibrium conditions were achieved as recommended by Hulme and Trevethick (2010). Cmpd-3 binds the α_{1A}-AR subtype with an approximate affinity of 100 nM when 0.5 mM GTP is added to the buffer and could not fully inhibit the binding of the radiolabeled antagonist, ^{125}I-HEAT (Fig. 2). When GTP is removed from the binding buffer, Cmpd-3 displays two binding affinity sites, typically seen with GPCR agonists, a high affinity site of 0.13 pM and a low affinity site of 54 nM (Fig. 3). The inability of Cmpd-3 to fully inhibit the radioligand ^{125}I-HEAT suggested that this compound could be an allosteric modulator. The ability of the orthosteric α_1-AR antagonist, phentolamine, and agonists, cirazoline and RO115-1224 (Fig. 1), to fully inhibit I^{125}-HEAT binding, demonstrate distinctive orthosteric effects (i.e. full inhibition) even though there are similarities in structure to Cmpd-3 (Fig. 2). Cmpd-3 did not display any binding towards the α_{1B}-AR subtype (Fig. S2) and low affinity binding at the α_{1D}-AR (K_i = 30 μM) (Fig. S3) showing a 1000-fold difference in binding selectivity between the subtypes. As imidazolines that are selective for the α_{1A}-AR also can bind to α_2-ARs, but display antagonistic and not agonistic function, we analyzed the ability of Cmpd-3 to inhibit the α_{2A}-AR using ^{3}H-RX821002 on membranes isolated from Cos-1 cells stably-expressing the α_{2A}-AR. Cmpd-3 displayed orthosteric binding at

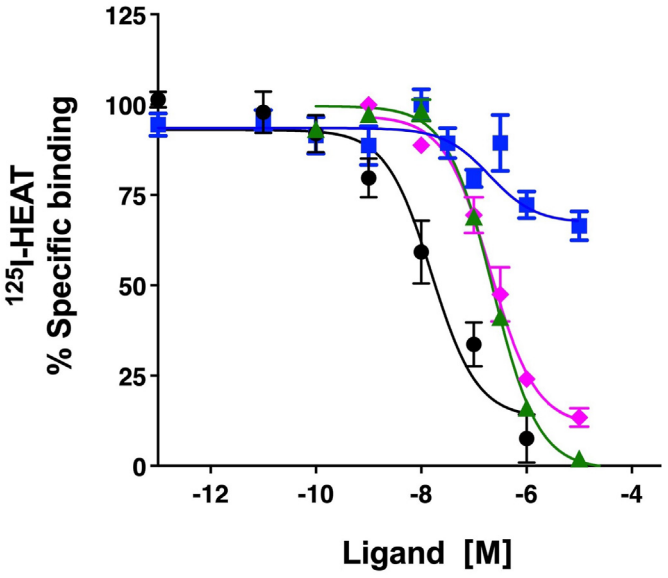

Fig. 2. Cmpd-3 binding at the α_{1A}-AR. Competition binding performed in membranes isolated from Rat-1 fibroblasts expressing the α_{1A}-AR and using the radiolabeled antagonist, ^{125}I-HEAT. In the presence of 0.5 mM GTP, Cmpd-3 showed an affinity of 30 nM for the α_{1A}-AR (blue squares) but with incomplete inhibition of ^{125}I-HEAT, suggesting allostery. The orthosteric ligands, phentolamine (black circles), cirazoline (green triangles) and RO115-120 (pink diamonds) completely inhibited ^{125}I-HEAT. N = 3–6 independent experiments performed in duplicate. Data was analyzed in GraphPad Prism using the one-site competitive binding algorithm. (For interpretation of the references to colour in this figure legend, the reader is referred to the Web version of this article.)

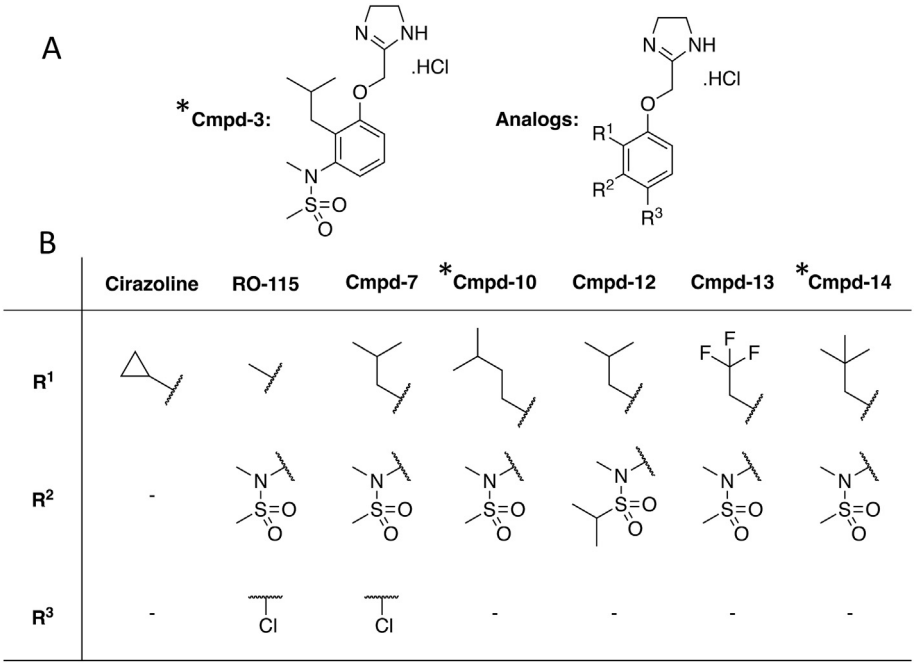

Fig. 1. Select Cmpd-3 derivations. (A) Structure of lead Compound 3 (Cmpd-3) and key substituents (R1-3) for structure-function analysis. (B) Structures of starting compound (i.e. cirazoline), the α_{1A}-AR agonist, RO115,1240 and key derivations. The different chemical structures substituted from Cmpd-3 are shown in the R1, R2, and R3 regions. * indicate PAMs.

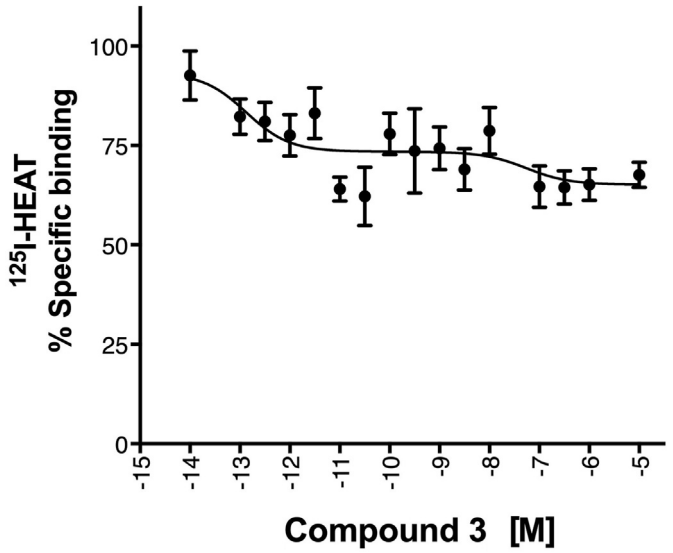

Fig. 3. Cmpd-3 displays high and low affinity sites in Rat-1 fibroblasts expressing the α_{1A}-AR. Competition binding performed in membranes isolated from Rat-1 fibroblasts expressing the α_{1A}-AR using the radiolabeled antagonist, ^{125}I-HEAT. When competition binding is performed without GTP, Cmpd-3 shows 2-binding sites, typically seen with agonists at GPCRs. A high affinity site of 0.13 pM and a low affinity site of 54 nM. N = 7 independent experiments. Data was analyzed in GraphPad Prism using the two-site competitive binding algorithm.

α_{2A}-ARs and fully inhibited ^{3}H-RX821002, similar to the control α_2-AR antagonist, rauwolscine, but with a much lower affinity of 130 mM (Fig. S4). A screen of 39 other class A GPCRs performed by the Psychoactive Drug Screening program (Besnard et al., 2012) reveal no other significant binding to other GPCRs except the 5-HT7A which had a K_i of 6 μM, still a 1000-fold lower affinity than at the α_{1A}-AR.

Cmpd-3 PAM activity is receptor, ligand, and signal-biased; potentiation of NE-mediated but not Epi-mediated cAMP. PAMs can allosterically stabilize the active conformation of a receptor enhancing downstream signal transduction in a manner similar to G-proteins (Langmead, 2011). A very common property of allosteric modulators is not only can they be specific for a receptor subtype but they can also impart signaling- and ligand-biased effects (Wootten et al., 2013). This was also the case for Cmpd-3. Cmpd-3 is not an agonist and is a pure PAM. It cannot stimulate inositol phosphate or cAMP second messengers by itself in a dose-response and was distinctively different from cirazoline and RO115-1224 which were both partial agonists at the α_{1A}-AR (Fig. 4). However, Cmpd-3 at nM concentrations potentiated the cAMP-mediated response of NE in the presence of the β-blocker, propranolol and rauwolscine, an α_2-AR blocker (Fig. 5A), but did not affect the cAMP-mediated response of Epi (Fig. 5B). Also confirming Cmpd-3's specificity for the α_{1A}-AR subtype only, there was no effect of Cmpd-3 on the NE or Epi-mediated cAMP response of either the α_{1B}- or α_{1D}-AR subtype (Fig. S5). Cirazoline and RO115-1224 displayed rightward curve-shifting effects consistent with a competitive partial agonist at both the NE- or Epi-mediated cAMP response (Fig. 5C–F) with cirazoline having greater intrinsic activity than RO115-1224 at the cAMP response. While Gq-coupling to IP signaling is considered the main signaling pathway for α_1-ARs, the ability of cirazoline and particularly, RO115-1224, a demonstrated highly-selective agonist for the α_{1A}-AR (Blue et al., 2004) to effect NE-mediated cAMP in the presence of a β-AR blocker indicates a true α_1-AR coupling to this pathway.

To assess if Cmpd-3 also had allosteric effects on another α_{1A}-AR mediated signal, we determined the ability of Cmpd-3 to alter the total inositol phosphate signal of NE or Epi. There was no effect of Cmpd-3 on either the NE or Epi-mediated IP signal at the α_{1A}-AR (Fig. 6AB) or on the

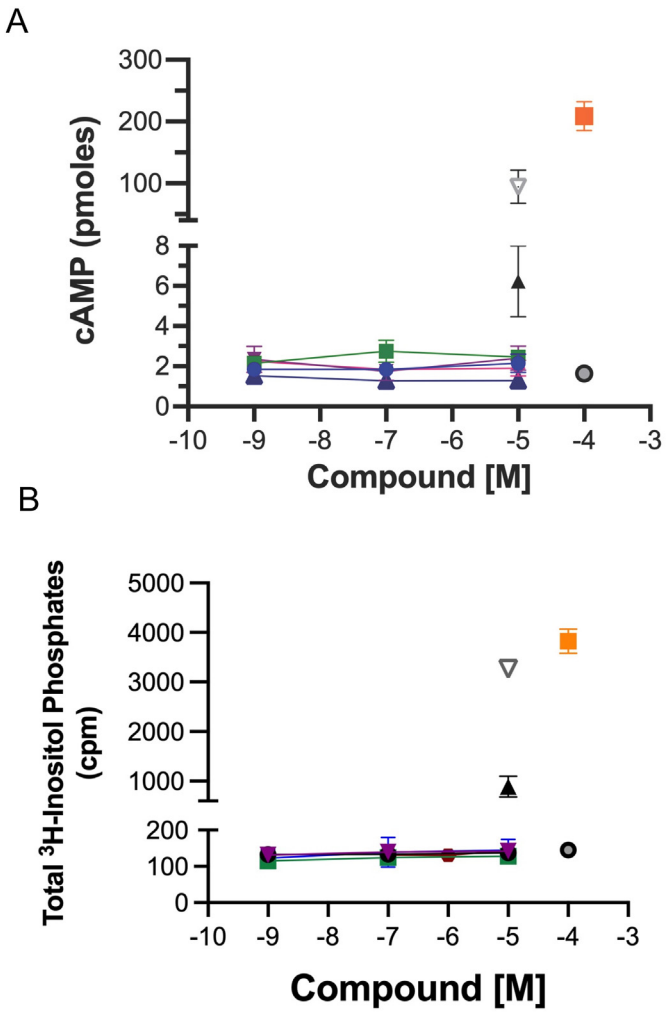

Fig. 4. Cmpd-3 has no intrinsic basal activity at either (A) cAMP or (B) IP signaling in Rat-1 fibroblasts expressing the α_{1A}-AR. Cmpd-3 (blue circles), Cmpd-10 (green squares), Cmpd-12 (purple triangles), Cmpd-13 (pink diamonds), and Cmpd-14 (blue triangles) do not show any basal activity. NE (10^{-4} M) alone (orange squares), Cirazoline (10^{-5} M) alone (grey triangles), RO115-1240 (10^{-5} M) alone (black triangles), and media alone (grey circles) serve as controls to illustrate full and partial agonists. N = 3–4 independent experiments performed in duplicate. (For interpretation of the references to colour in this figure legend, the reader is referred to the Web version of this article.)

α_{1B}- or α_{1D}-AR subtypes (data not shown). Cirazoline and RO115-1224 again displayed rightward curve-shifting effects consistent with a competitive partial or full agonist behavior at both the NE- or Epi-mediated IP response (Fig. 6C–F). Overall, these results indicate that Cmpd-3 is a PAM that is specific for the α_{1A}-AR subtype and is both ligand and signal-biased.

Cmpd-3 potentiates the phosphorylation of p-CREB. To confirm effects of Cmpd-3 on the NE-mediated cAMP signal, we next assessed the phosphorylation levels of the cAMP response element-binding protein (CREB) at Ser133. p-CREB activity activates many gene targets in response to higher cAMP levels, particularly in NE-mediated memory formation and its retrieval (Kabitzke et al., 2011; Huang et al., 2017; Bartolotti and Lazarov, 2019). In corroboration with potentiated cAMP levels, Cmpd-3 (10^{-8} M) also significantly potentiated NE-mediated p-CREB levels even when β- and α_2-AR receptors were blocked (Fig. 7).

Cmpd-3 stabilizes high affinity state. Since Cmpd-3 potentiated only the NE-specific cAMP signal, we next assessed whether Cmpd-3 altered the binding characteristics of NE at the α_{1A}-AR. In the absence of GTP, NE

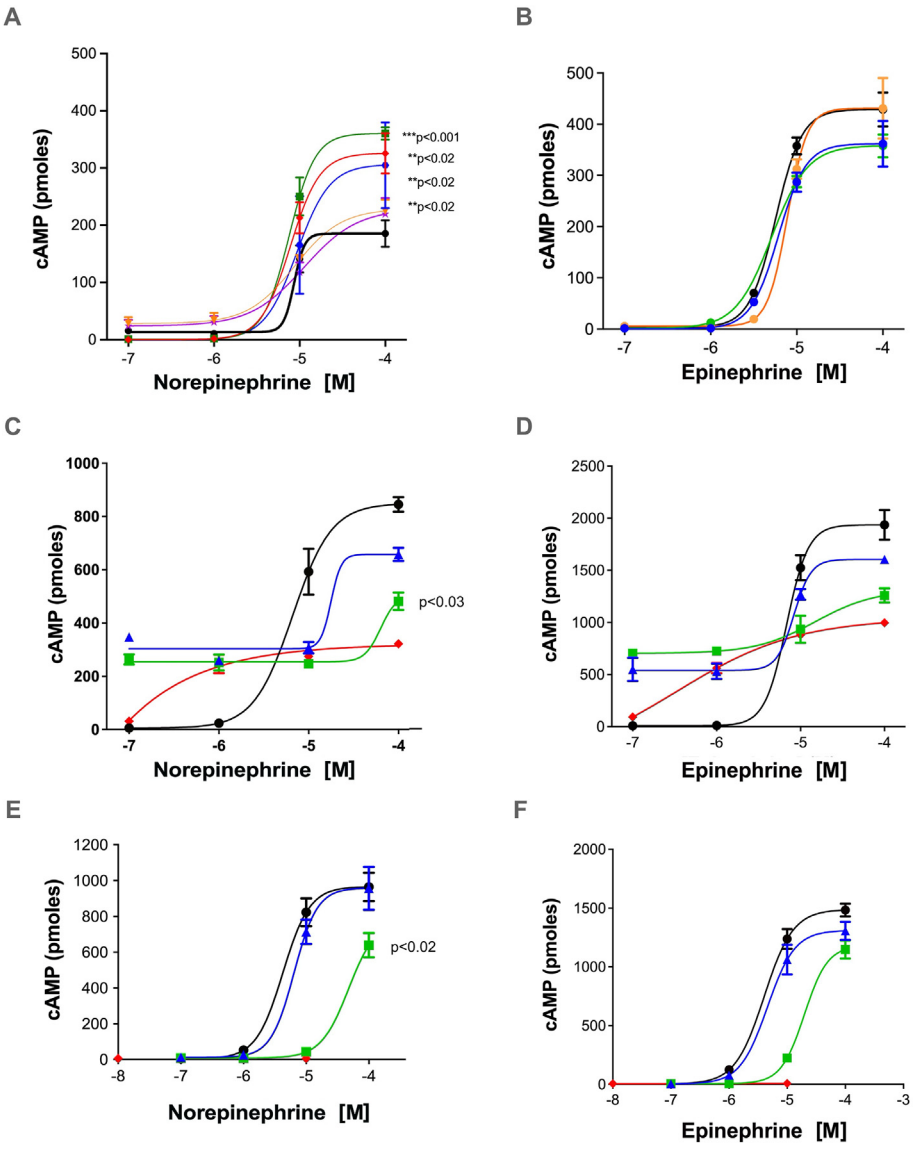

Fig. 5. Cmpd-3 potentiates the NE-mediated (A) but not the Epi-mediated (B) cAMP signaling in Rat-1 fibroblasts expressing the α_{1A}-AR. Cmpd-3 (red diamonds, 10^{-8} M; green squares, 10^{-9} M; blue hexagons,10^{-10} M; gold triangles, 10^{-7} M; purple stars, 10^{-6} M) increases the Emax of the cAMP signaling when added to NE (A) but not Epi (B) compared to NE or Epi alone (black circles). Cirazoline (C–D) nor RO 115–1240 (E–F) (green squares, 10^{-5} M; blue triangles, 10^{-6} M) displayed rightward shifting competitive effects when added to NE or EPI (alone, black circles). Cirazoline or RO 115–1240 alone (red diamonds). N = 3–7 independent experiments performed in duplicate. (For interpretation of the references to colour in this figure legend, the reader is referred to the Web version of this article.)

displays two binding sites of high and low affinity (K_{iH} −8.5; K_{iL} −5) with 15% of the receptor in the high affinity state conformation. The presence of Cmpd-3 (10^{-5} M) increased the fraction of receptor in the high affinity state (55%). In contrast, the same dose (10^{-5} M) of cirazoline fully-inhibited the binding of NE in a competitive manner (Fig. 8A). There was no effect of Cmpd-3 on the binding profile of Epi (Fig. 8B). There were similar effects on NE-binding when cmpd-14 was used. To confirm effects of Cmpd-3 to stabilize the high affinity site of NE, Cmpd-3 could dose-dependently increase the binding of radiolabeled ^{3}H-NE to the α_{1A}-AR when a constant amount of ^{3}H-NE was added equaled to the high affinity state of NE (42 nM) (Fig. 9). The binding effect of Cmpd-3 also saturated, typical of allosteric modulators. Together with the signal assays, these studies indicate that Cmpd-3 stabilizes the NE-mediated active state conformation of the α_{1A}-AR leading to potentiation of signaling but also a conformation that favors the formation of cAMP.

PAM assay development in primary and transfected cell lines. A PAM assay has been developed that shows the dose-dependency, Emax, and potency (EC_{50}) of Cmpd-3's response to NE-mediated cAMP potentiation in transfected Rat-1 fibroblasts (Fig. 10A), transformed human neuroblastoma SK-N-MC cell line (Fig. 10B), or primary mouse cardiomyocytes (Fig. 10C). In this assay, the concentration of NE is held constant at its Emax (10^{-4} M) (Fig. 10, red line). Cmpd-3 is then added in a dose-response (Fig. 10, blue line). Any signal above the red line is potentiation. For Cmpd-3, the Emax is potentiated by 35–60% over NE's maximum response alone. The signal stays elevated (i.e. ceiling effect), common with PAMs, then begins to wane at higher concentrations of Cmpd-3, suggesting desensitization (Hellyer et al., 2019) or competitive binding to the orthosteric site. The potency of Cmpd-3 to potentiate the NE-mediated cAMP response is consistent with the high affinity site of Cmpd-3 binding to the α_{1A}-AR (Fig. 3). The different values for Emax and EC_{50} depend upon the cell line used and the amount of receptor reserve, where low receptor reserve shifts the curve to the right as shown in primary adult cardiomyocytes (Fig. 10B). However, when receptors are vastly overexpressed (1000+-fold over endogenous G-proteins levels), we could not detect PAM activity as most of the receptors are uncoupled from the G-protein.

Cmpd-3 structure-function. To assess some of the key structural determinants of PAM activity, we also analyzed derivatives with changes in the *ortho*- or *para*-substituent groups. Extending the carbon chain in the *ortho*-isopentyl group (Fig. 1, Cmpd-10), or adding an additional methyl to form a tert-butyl group (Fig. 1, Cmpd-14) retained PAM activity, while substituting fluorine for carbon in Cmpd-14 (Fig. 1, Cmpd-13), lost PAM activity (Fig. 11). Modification of the sulfonamide *S*-methyl of Cmpd-3 to *iso*-propane (Fig. 1, Cmpd-12) also lost PAM activity. Adding a *para*-

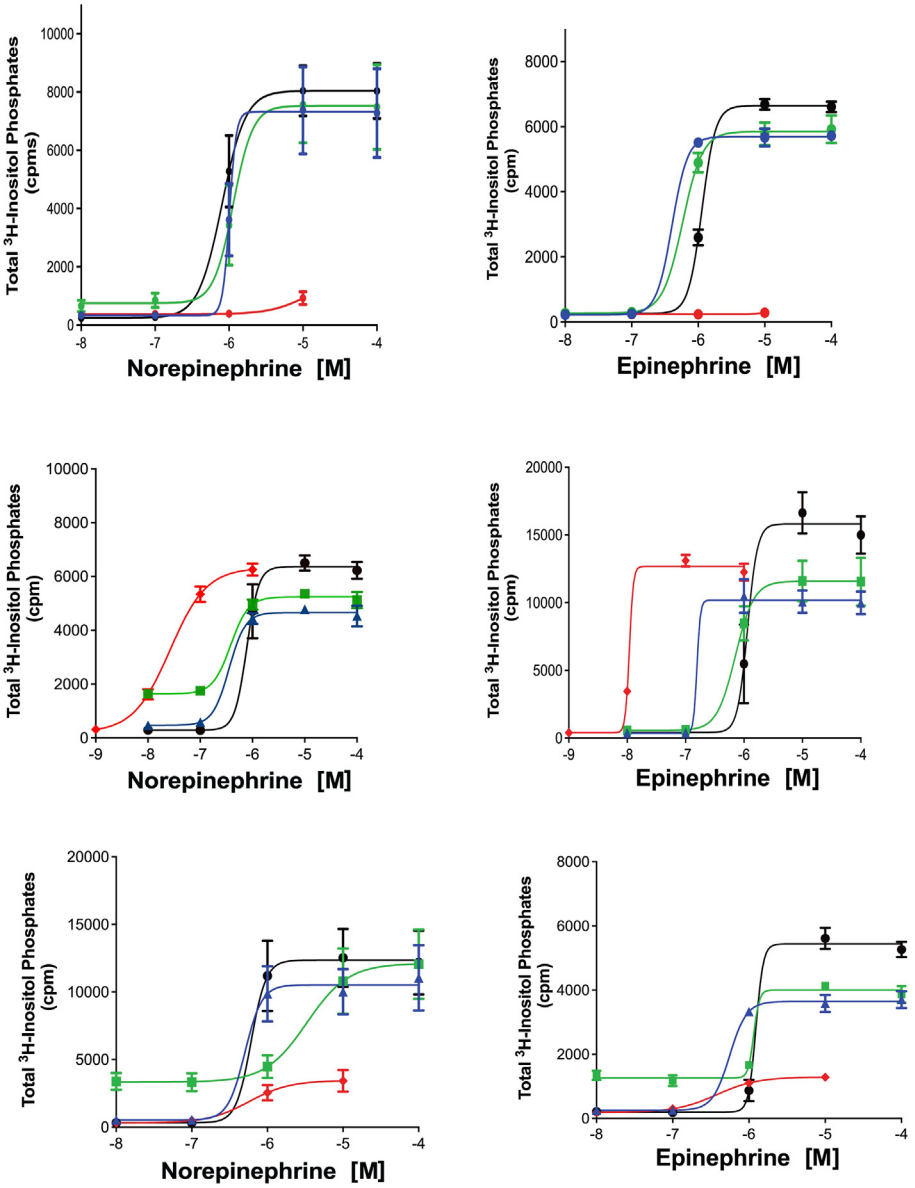

Fig. 6. Cmpd-3 does not affect the NE-mediated (A) nor the Epi-mediated (B) inositol phosphate signaling in Rat-1 fibroblasts expressing the α_{1A}-AR. Cmp-3 (green circles,10^{-5} M; blue circles,10^{-7} M) when added to NE (A) or Epi (B) does not affect inositol phosphate signaling compared to NE or Epi alone (black circles). Cmpd-3 alone (red diamonds). (C) Cirazoline (green squares,10^{-7} M; blue triangles,10^{-8} M), or (D) Cirazoline (green squares,$10^{-8.5}$M; blue triangles,10^{-9} M), or (E, F) RO115-1240 (green squares,10^{-5} M; blue triangles,10^{-7} M) displayed effects consistent with a partial or full agonist when added to NE or EPI (alone, black circles). Cirazoline or RO 115–1240 alone (red diamonds). N = 3–4 independent experiments performed in duplicate. (For interpretation of the references to colour in this figure legend, the reader is referred to the Web version of this article.)

chloro to Cmpd-3, mimicking RO115-1224, also lost PAM activity (data not shown). Cmpds-12 and -13 displayed competitive effects on NE-mediated cAMP at higher concentrations similar to cirazoline (Fig. 11).

4. Discussion

We have developed the first series of novel small molecular weight compounds that are PAMs at the α_{1A}-AR. These compounds were first derivatized from the imidazoline agonist, cirazoline. Imidazoline agonists display better brain penetrance, inherent α_{1A}-AR selectivity, and biased signaling to cAMP pathways compared to α_{1A}-AR phenethylamine agonists, such as methoxamine (Evans et al., 2011; da Silva Junior et al., 2017). These PAMs are selective for the α_{1A}-AR subtype, displaying poor or absent binding and/or signaling effects at the α_{1B}- or α_{1D}-AR subtypes (Figs. S2–4). A high affinity binding site (pM) is consistent with agonistic G-protein allosteric behavior and sub nM potency seen in signal transduction PAM assays (Fig. 10) and with nM Emax observed *in vivo* on cognitive and memory effects (Perez, 2021b; in preparation). The high affinity Ki measurement we observed (0.13 pM) are obtained from algorithms and based upon shallow curves and may not be absolute. Allosteric modulators such as cmpd-3 can have additional allosteric effects depending upon the ligand used, the amount of receptor pre-coupled to G-protein (based upon the degree of overexpression), and with possible interactions with the lipid environment (Szlenk et al., 2021) that can alter observed affinity.

Cmpd-3 was studied extensively and found also to be both ligand and signal-biased, a common property of PAMs (Kenakin, 2005; Valant et al., 2012). They effect both the binding and signaling properties of the NE-bound receptor but have no effects on the Epi-bound receptor. Cmpd-3 is a pure PAM and does not display any basal agonist activity, yet Cmpd-3 biased and potentiated cAMP signaling (Fig. 5) and the cAMP-mediated transcription factor p-CREB (Fig. 7), without effects on the IP response (Fig. 6). NE mediates the cognitive effects of ARs through cAMP signaling utilizing both α_1-and β-ARs (Ferry et al., 1999a,b; Hatfield and McGaugh, 1999) and through p-CREB activity (Kabitzke et al., 2011; Huang et al., 2017).

While the IP response is the canonical second messenger activated by the α_1-AR through Gq coupling, cAMP signaling has been documented and particularly biased with α_{1A}-AR selective imidazolines (Evans et al., 2011; da Silva Junior et al., 2017), through either a PKA-dependent (Lin et al., 1998; Markou et al., 2004; Gallego et al., 2005; Scarparo et al., 2006; Sugimoto et al., 2011), PKC-dependent (Thonberg et al., 2002), or

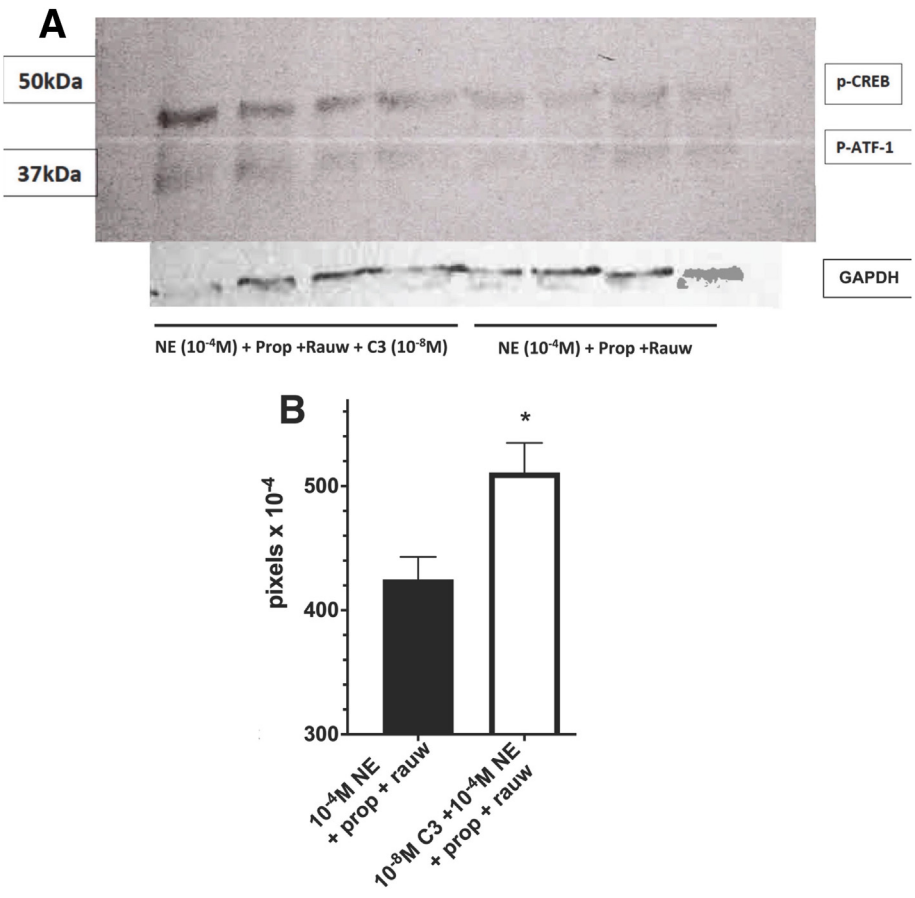

Fig. 7. Cmpd-3 increases NE-mediated phosphorylation of CREB in the presence of α_2-and β-AR blockers. (A) Western blot analysis of pSer133-CREB levels in rat-1 fibroblasts transfected with the α_{1A}-AR. Cells were preincubated for 2 h with β-AR inhibitor, propranolol (10 μM) and the α_2-AR inhibitor rauwolscine (0.1 μM), with or without the addition of Cmpd-3 (10^{-8} M) in the presence of 500 μM IBMX. Cells were stimulated by NE (10^{-4} M) for an additional 2 h before subjected to SDS-PAGE. The transferred blot was probed with rabbit p-CREB antibody (pSer133, Cell Signaling #9198) at 1:1000, then 1:10,000 goat anti-rabbit IgG HRP in 5% BSA in PBST. The blot was stripped and incubated with rabbit GAPH antibody (Cell Signaling # 2118) as a loading control. (B) The bands were quantified using the Image Studio Digits Version 4.0 program associated with the Li-Cor digital scanner model C-DIGit, normalized to GAPDH, and graphed using Prism software. P-CREB is identified at 43 kDa, and a phosphorylated form of the CREB-related protein ATF-1 also cross reacts (29 kDa). pRepresentative gel. N = 12, from 3 independent experiments performed in quadruplet. *P < 0.008.

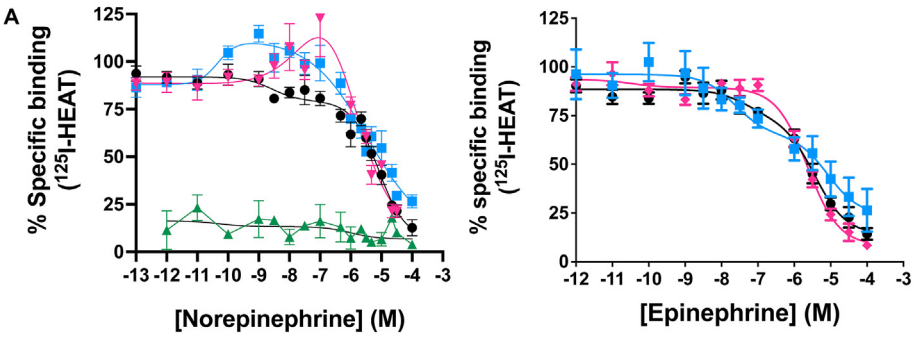

Fig. 8. Cmpd-3 stabilizes the high affinity binding site of NE but not Epi. Competitive binding was performed in membranes isolated from Rat-1 fibroblasts expressing the α_{1A}-AR and using ^{125}I-HEAT as the radiolabel and in the absence of GTP to display two-site binding typical of GPCR agonists. **A)** Competition binding of NE at the α_{1A}-AR (black circles) or in the presence of Cmpd-3 (10^{-5} M)(blue squares) or cmpd-14(10^{-5} M)(red triangles). Same dose of the allosteric partial agonist, cirazoline (10^{-5} M), binds to orthosteric site as NE and completely competes off NE binding (green triangles). (B) Competition binding curve of Epi at the α_{1A}-AR (black circles) competing off the radiolabel antagonist ^{125}I-HEAT with a 10^{-5} M dose of Cmpd-3 (blue squares) or cmpd-14 (red diamonds). N = 4–8 independent experiments performed in duplicate. Data was analyzed in GraphPad Prism using the one or two-site competitive binding algorithm. (For interpretation of the references to colour in this figure legend, the reader is referred to the Web version of this article.)

indirect pathways (Harley et al., 2006) depending upon the cell type. In fact, we demonstrated that Cmpd-3 potentiates a major downstream effector of NE-mediated cAMP signaling, p-CREB (Fig. 7). In addition, as the IP response activates PKC which is not altered by Cmpd-3, it is unlikely that CREB phosphorylation was increased via PKC.

Radioligand binding studies also confirm the allosteric interaction of Cmpd-3. A saturating concentration of the orthosteric agonist cirazoline (10^{-5} M) can compete at the same binding site as NE, causing complete inhibition of the radiolabel ^{125}I-HEAT. In contrast, Cmpd-3 at the same concentration as cirazoline did not compete but increased the fraction of receptor in the high affinity state (Fig. 8), suggesting that cmpd-3 stabilizes or promotes the active-state conformation. These results were confirmed when a dose response of Cmpd-3 increased the binding of a 42 nM concentration of ^{3}H-NE (Fig. 9), which would only occupy the high affinity site of NE at the α_{1A}-AR. There was no effect of Cmpd-3 on the binding properties of Epi. Interestingly, there was increased binding of ^{125}I-HEAT when either cmpd-3 or cmpd-14 was added to the NE-bound receptor (Fig. 8A). Comparison to Epi-binding curves (Fig. 8b) indicates that the effect is NE-specific. The increase in ^{125}I-HEAT binding was NE-bound receptor specific and could be due to allosteric effects on

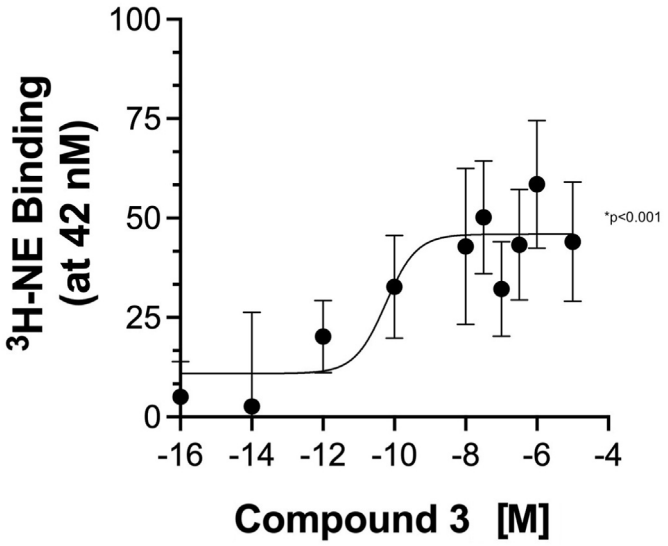

Fig. 9. Cmpd-3 dose-dependently potentiates the binding of ^{3}H-NE at its high affinity site. Binding experiments were performed in membranes isolated from Rat-1 fibroblasts expressing the α_{1A}-AR and using the radiolabeled agonist, ^{3}H-NE at a single dose of 42 nM, its high affinity site. Cmpd-3 dose-dependently increased the amount of ^{3}H-NE bound to the α_{1A}-AR with a potency of 0.1 nM. N = 7 independent experiments performed in duplicate.

receptor expression, stability, or on ^{125}I-HEAT binding. There is precedent for altered receptor surface expression in the literature with allosteric modulators upon prolonged exposure (May et al., 2005; Sinner et al., 2019) as our binding assays are 5 h long. As alternate explanation is that the cmpd-3/NE complex may have an allosteric and conformational effect on ^{125}I-HEAT binding kinetics. Nevertheless, these results suggest that Cmpd-3 stabilizes the high-affinity G-protein bound state of NE (i.e. presumably by increasing residence time) (Cao et al., 2021), leading to the increased in signal transduction but with a conformation that is biased towards cAMP. While a ceiling effect of Cmpd-3, typical of PAMs (Wootten et al., 2013; Christopoulos, 2014), was seen in binding (Fig. 9), the PAM signaling assay (Fig. 10) showed inhibition at high concentrations which suggests a desensitization of the signal. Alternately, high concentrations of the PAM might begin to bind at the orthosteric binding site, leading to competitive effects.

While Cmpd-3 is novel, it does share some structural similarities to RO115-1240 and cirazoline (Fig. 1). However, neither RO115-1240 nor cirazoline displayed any PAM characteristics, both having intrinsic agonist activity and demonstrate competitive effects with NE or EPI, consistent with a partial or full agonist at the α_{1A}-AR. There are two types of PAMs currently described in the literature (type I & type II) (Hackos and Hanson, 2017; Allegretti et al., 2016; Targowska-Duda et al., 2018). Type I PAMs can enhance maximum activity without altering EC_{50} and are conformationally driven while type II PAMs act by shifting the EC_{50} to higher affinity with little effect on maximum activity. There are also mixed type I/II PAMs. Cmpd-3 appears to be consistent as a Type I PAM via potentiation of the cAMP maximal response without altering the affinity of the receptor.

Through structure-function analysis, we were able to discern some patterns of the structural determinants for PAM activity at the α_{1A}-AR. The R1 position (Fig. 1A) was previously shown to impart α_{1A}-AR agonist selectivity when occupied by aliphatic hydrophobic groups (Hwa et al., 1995). The R2 position through hydrogen bonding imparts signaling efficacy at the α_{1A}-AR with little effect on binding (Hwa and Perez, 1996) but cirazoline is a noted exception. While the R3 position in the α_{1A}-AR can accommodate bulk which contributes to binding selectivity, it is not a major contributor (McCune et al., 2004). We hypothesized that the interaction and packing of R1 and R2 accounts for the PAM activity as

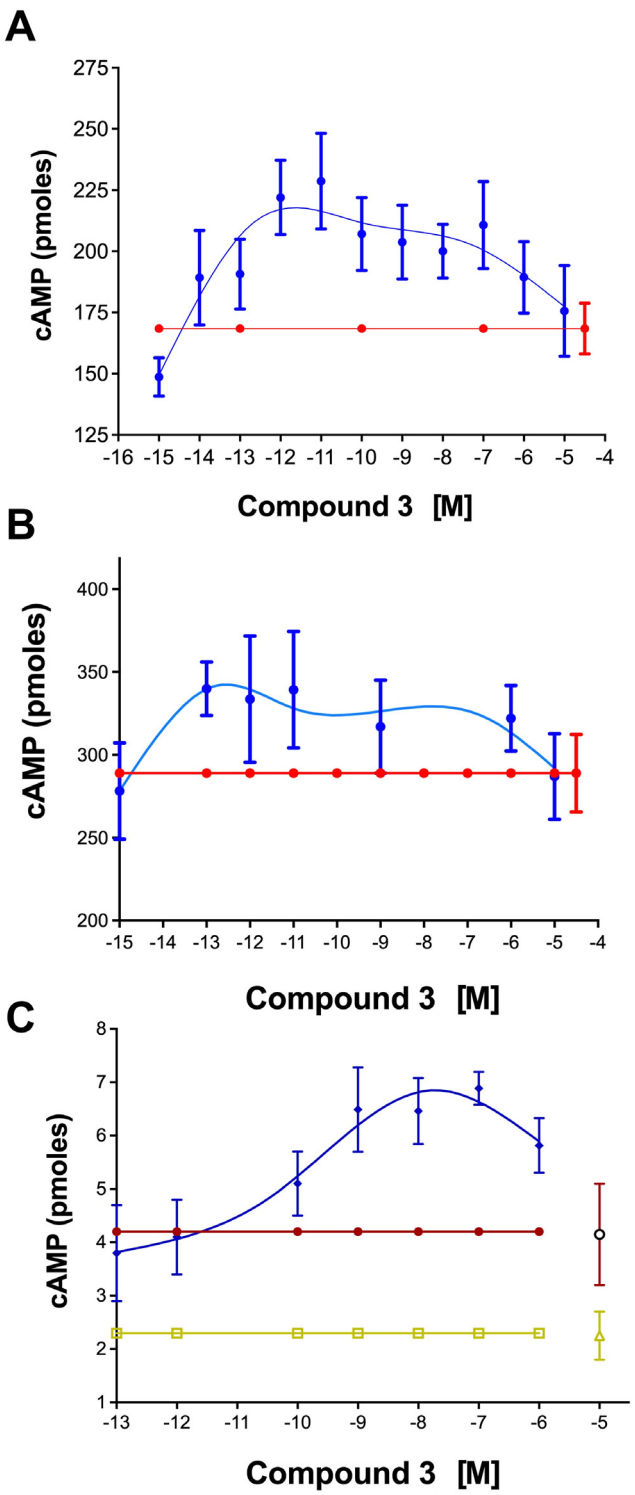

Fig. 10. Cmpd-3 can potentiate the NE-mediated cAMP response in transfected Rat-1 fibroblasts (A), human SK-N-MC, a transformed neuroblastoma cell line (B) or primary mouse cardiomyocytes in a PAM assay (C). To show PAM effects of potency and Emax, the concentration of NE is held constant at its Emax (10^{-4} M) (red line). Cmpd-3 is then added in a dose-response (blue line). Any signal above the red line is potentiation. Cmpd-3 potentiates the NE-mediated cAMP response with a potency of 0.1 pM in neuroblastoma cells (A) or 0.5 nM in primary cardiomyocytes (B). Media alone (yellow squares). The shift to the right in the primary cells is due to endogenous receptor density. N = 4(C); 6(B); 13(A) independent experiments. (For interpretation of the references to colour in this figure legend, the reader is referred to the Web version of this article.)

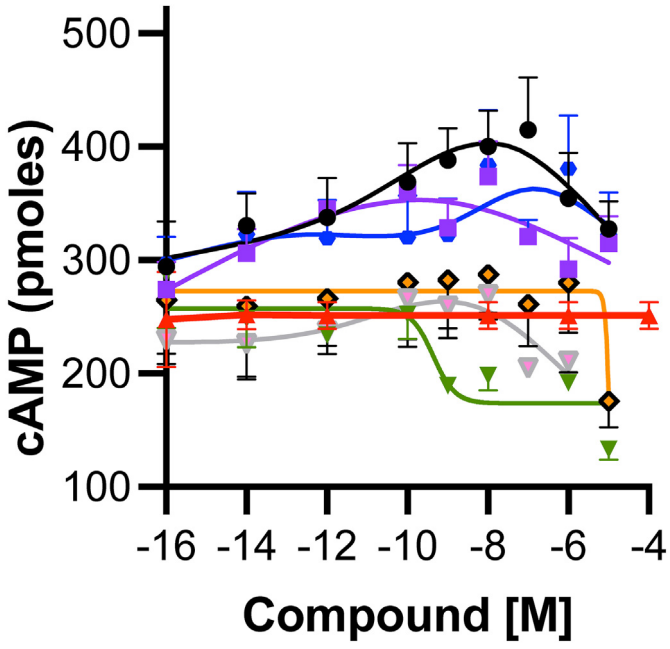

Fig. 11. Cmpds-3,-10,-14 display PAM effects of NE-mediated cAMP potentiation in Rat-1 fibroblasts expressing the α_{1A}-AR. To show PAM effects of potency and Emax, the concentration of NE is held constant at its Emax (10^{-4} M) (red triangles). Various Cmpds are then added in a dose-response. Any signal above the red line is potentiation, below the red line is competitive inhibition. Cmpds-3, 10 and 14 display PAM effect while Cmpds-12 and 13 display competitive inhibition similar to the orthosteric partial agonist cirazoline. NE + Cmpd-3 (black circles), NE + Cmpd-10 (blue circles), NE + Cmpd-12 (pink triangles), NE + Cmpd-13 (orange diamonds), NE + Cmpd-14 (purple squares), NE + cirazoline (green triangles). N = 3–6 independent experiments performed in duplicate. (For interpretation of the references to colour in this figure legend, the reader is referred to the Web version of this article.)

increasing the carbon length or hydrophobic bulk in the R1 as in Cmpds-10 and 14 result in PAM activity, but substitution of fluorine for carbons in the R1 isobutane of Cmpd-13 abolishes PAM activity (Fig. 1). Likewise, substitution of the R2 methyl sulfonamide to *iso*-propyl in Cmpd-12 also abolished PAM activity. Interestingly, simply adding a chlorine substituent at R3 to Cmpd-3, similar to RO115-1240, also abolished PAM activity (Cmpd-7). We speculate that since chlorine is electron withdrawing on an aromatic ring, the hydrogen bonding and resulting binding effects of Cmpd-3's R2 methyl-methane sulfonamide may have been changed that reduced its affinity for the allosteric binding pocket. Further structure-function analysis is required to substantiate this.

Cmpd-3 and its analogs are the first PAMs described for the α_1-AR family. There have been negative allosteric modulators previously reported for the α_1-and α_2-ARs (Leppik et al., 2000; Leppik and Birdsall, 2000; Sharpe et al., 2003; Campbell et al., 2017). PAMs have been described for the GPCR adrenergic-related, β_2-AR (Ahn et al., 2018) as well as many other more distantly-related GPCRs (Canals et al., 2012; Chan et al., 2008; Kruse et al., 2013). Because of signal-selectivity for only the cAMP signaling of NE at the α_{1A}-AR, with no intrinsic activity nor effects on the IP signal, it is hypothesized that there will be no effect of Cmpd-3 on blood pressure. This hypothesis has been substantiated in part from our prior genetic phenotype, *in vivo* (Perez, 2021b). Cmpd-3 (2.6 mg/kg, q.d., PO) at either 3 months or 6 months of dosing failed to change systolic blood pressure in 3XTG mice but statistically increased long-term potentiation and cognitive behavior (Perez, 2021b). Without effects on blood pressure, Cmpd-3 and its analogs may provide a superior therapeutic strategy to treat Alzheimer's Disease (Perez, 2020, 2021a,b) and/or heart failure (Perez, 2020, 2021a,c).

In summary, we have characterized the first discovery of a PAM for the α_{1A}-AR. These PAMs displays high selectivity and cAMP signal-bias for the α_{1A}-AR but only with the NE-bound conformation. Its ability to modulate NE but not Epi binding and only cAMP signaling would target effects in the brain, lessen or eliminate blood pressure and other side effects, making it a desirable therapeutic for neurological diseases.

CRediT authorship contribution statement

Robert S. Papay: Methodology, Validation, Formal analysis, Data curation, Writing – original draft, Visualization. **Jonathan D. Macdonald:** Methodology, Validation, Investigation, Resources, Data curation, Writing – original draft. **Shaun R. Stauffer:** Conceptualization, Methodology, Investigation, Resources, Writing – review & editing, Visualization. **Dianne M. Perez:** Conceptualization, Methodology, Validation, Formal analysis, Investigation, Resources, Data curation, Writing – original draft, Writing – review & editing, Visualization, Supervision, Funding acquisition.

Declaration of competing interest

The authors declare the following financial interests/personal relationships which may be considered as potential competing interests: The authors have filed the following patents: PCT/US2020/029583, filed 4/23/2020. European Patent (No. 20794530.4) filed 10/15/2021. US utility (17/605,801) filed 10/21/2021.Inventors: PEREZ, Dianne M.; STAUFFER, Shaun R.; MACDONALD, Jonathan. Allosteric Activators of the Alpha1A-Adrenergic receptor.

Data availability

Data will be made available on request.

Acknowledgements

Cos-1 cells stably-expressing the α_1-ARs was a gift from GlaxoSmithKline and the stably-expressing α_{2A}-AR cell line was a gift from Rick Neubig. This work was supported by grants from the National Institute of Aging RO1-AG066627 and R03AG049394, The Edward N. & Della L. Thome Memorial Foundation Awards Program in Alzheimer's Disease Drug Discovery Research, the BrightFocus Foundation, and the ADDF-Harrington Scholar Program to D.M.P.

Appendix A. Supplementary data

Supplementary data to this article can be found online at https://doi.org/10.1016/j.crphar.2022.100142.

References

Ahn, S., Kahsai, A.W., Pani, B., Wang, Q.T., Zhao, S., Wall, A.L., et al., 2017. Allosteric "beta-blocker" isolated from a DNA encoded small molecule library. Proc. Natl. Acad. Sci. U.S.A. 114, 1708–1713.

Ahn, S., Pani, B., Kahsai, A.W., Olsen, E.K., Husemoen, G., Vestergaard, M., et al., 2018. Small-Molecule positive allosteric modulators of the β_2-adrenoceptor isolated from DNA-encoded libraries. Mol. Pharmacol. 94 (2), 850–861.

Allegretti, M., Cesta, M.C., Locati, M., 2016. Allosteric modulation of chemoattractant receptors. Front. Immunol. 7, 170.

Bartolotti, N., Lazarov, O., 2019. CREB signals as PBMC-based biomarkers of cognitive dysfunction: a novel perspective of the brain-immune axis. Brain Behav. Immun. 8, 9–20. https://doi.org/10.1016/j.bbi.2019.01.004.

Besnard, J., Ruda, G.F., Setola, V., Abecassis, K., Rodriguiz, R.M., Huang, X.P., et al., 2012. Automated design of ligands to polypharmacological profiles. Nature 492 (7428), 215–220.

Bishop, M.J., 2007. Recent advances in the discovery of α_1-adrenoceptor agonists. Curr. Top. Med. Chem. 7, 135–145.

Blue, D.R., Daniels, D.V., Gever, J.R., Jett, M.F., O'Yang, C., Tang, H.M., et al., 2004. Pharmacological characteristics of Ro 115-1240, a selective $\alpha_{1A/1L}$-adrenoceptor partial agonist: a potential therapy for stress urinary incontinence. BJU Int. 93 (1), 162–170.

Campbell, A.P., Wakelin, L.P., Denny, W.A., Finch, A.M., 2017. Homobivalent conjugation increases the allosteric effect of 9-aminoacridine at the α_1-adrenergic receptors. Mol. Pharmacol. 91 (2), 135–144.

Canals, M., Lane, J.R., Wen, A., Scammells, P.J., Sexton, P.M., Christopoulos, A., 2012. A Monod-Wyman-Changeux mechanism can explain G protein-coupled receptor (GPCR) allosteric modulation. J. Biol. Chem. 287, 650–659.

Cao, A.M., Quast, R.B., Fatemi, F., Rondard, P., Pin, J.-P., Margeat, E., 2021. Allosteric modulators enhance agonist efficacy by increasing the residence time of a GPCR in the active state. Nat. Commun. 12, 5426.

Chan, W.Y., McKinzie, D.L., Bose, S., Mitchell, S.N., Witkin, J.M., Thompson, R.C., et al., 2008. Allosteric modulation of the muscarinic M4 receptor as an approach to treating schizophrenia. Proc. Natl. Acad. Sci. U.S.A. 105, 10978–10983.

Christopoulos, A., 2014. Advances in G protein-coupled receptor allostery: from Function to structure. Mol. Pharmacol. 86, 463–478.

Christopoulos, A., Kenakin, T., 2002. G protein-coupled receptor allosterism and complexing. Pharmacol. Rev. 54 (2), 323–374.

Collette, K.M., Zhou, X.D., Amoth, H.M., Lyons, M.J., Papay, R.S., Sens, D.A., et al., 2014. Long-term α_{1B}-adrenergic receptor activation shortens lifespan while α_{1A}-adrenergic receptor stimulation prolongs lifespan in association with decreased cancer incidence. Age 36, 9675–9677.

da Silva Junior, E.D., Sato, M., Merlin, J., Broxton, N., Hutchinson, D.S., Ventura, S., et al., 2017. Factors influencing biased agonism in recombinant cells expressing the human α_{1A} -adrenoceptor. Br. J. Pharmacol. 174 (14), 2318–2333.

Doze, V.A., Papay, R.S., Collette, K.M., Gupta, M.K., Lyons, M.J., Davis, B.A., et al., 2011. Long term α_{1A}-adrenergic receptor stimulation improves synaptic plasticity, cognitive function, mood and longevity. Mol. Pharmacol. 80 (4), 747–758.

Evans, B.A., Broxton, N., Merlin, J., Sato, M., Hutchinson, D.S., Christopoulos, A., Summers, R.J., 2011. Quantification of functional selectivity at the human α_{1A}-adrenoceptor. Mol. Pharmacol. 79 (2), 298–307. Erratum in: Mol Pharmacol. 2011 Mar;79(3):627.

Ferry, B., Roozendaal, B., McGaugh, J.L., 1999a. Involvement of α_1-adrenoceptors in the basolateral amygdala in modulation of memory storage. Eur. J. Pharmacol. 372, 9–16.

Ferry, B., Roozendaal, B., McGaugh, J.L., 1999b. Basolateral amygdala noradrenergic influences on memory storage are mediated by an interaction between β- and α_1-adrenoceptors. J. Neurosci. 19, 5119–5123.

Gallego, M., Setién, R., Puebla, L., Boyano-Adánez Mdel, C., Arilla, E., Casis, O., 2005. α_1-Adrenoceptors stimulate a Gαs protein and reduce the transient outward K+ current via a cAMP/PKA-mediated pathway in the rat heart. Am. J. Physiol. Cell Physiol. 288 (3), C577–C585.

Gupta, M.K., Papay, R.S., Jurgens, C.W.D., Gaivin, R.J., Shi, T., Doze, V.A., Perez, D.M., 2009. α_1-Adrenergic receptors regulate neurogenesis and gliogenesis. Mol. Pharmacol. 76 (2), 314–326.

Hackos, D.H., Hanson, J.E., 2017. Diverse modes of NMDA receptor positive allosteric modulation: mechanisms and consequences. Neuropharmacology 112, 34–45.

Harley, C.W., Darby-King, A., McCann, J., McLean, J.H., 2006. β_1-adrenoceptor or α_1-adrenoceptor activation initiates early odor preference learning in rat pups: support for the mitral cell/cAMP model of odor preference learning. Learn. Mem. 13 (1), 8–13.

Hatfield, T., McGaugh, J.L., 1999. Norepinephrine infused into the basolateral amygdala enhances spatial water maze memory. Neurobiol. Learn. Mem. 71, 232–239.

Hellyer, S.D., Albold, S., Sengmany, K., Singh, J., Leach, K., Gregory, K.J., 2019. Metabotropic glutamate receptor 5 ($mGlu_5$)-positive allosteric modulators differentially induce or potentiate desensitization of $mGlu_5$signaling in recombinant cells and neurons. J. Neurochem. 151 (3), 301–315.

Huang, B., Zhu, H., Zhou, Y., Liu, X., Ma, L., 2017. Unconditioned- and conditioned-stimuli induce differential memory reconsolidation and β-AR-dependent CREB activation. Front. Neural Circ. 11, 53. https://doi.org/10.3389/fncir.2017.00053.

Hulme, E.C., Trevethick, M.A., 2010. Ligand binding assays at equilibrium: validation and interpretation. Br. J. Pharmacol. 161 (6), 1219–1237.

Hwa, J., Graham, R.M., Perez, D.M., 1996. Chimeras of α_1-adrenergic receptor subtypes identify critical residues that modulate active-state isomerization. J. Biol. Chem. 271, 7956–7964.

Hwa, J., Graham, R.M., Perez, D.M., 1995. Identification of critical determinants of α_1-adrenergic receptor subtype selective agonist binding. J. Biol. Chem. 270 (39), 23189–23195.

Hwa, J., Perez, D.M., 1996. The unique nature of the serine interactions for a1-adrenergic receptor agonist binding and activation. J. Biol. Chem. 271 (11), 6322–6327.

Kabitzke, P.A., Silva, L., Wiedenmayer, C., 2011. Norepinephrine mediates contextual fear learning and hippocampal pCREB in juvenile rats exposed to predator odor. Neurobiol. Learn. Mem. 96 (2), 166–172. https://doi.org/10.1016/j.nlm.2011.04.003, 2011 Sep.

Kenakin, T., 2005. New concepts in drug discovery: collateral efficacy and permissive antagonism. Nat. Rev. Drug Discov. 4, 919–927.

Kiowski, W., Bolli, P., Erne, P., Müller, F.B., Hulthén, U.L., Bühler, F.R., 1989. Mechanisms of action and clinical use of calcium antagonists in hypertension. Circulation 80 (6 Suppl. I), IV136–I144.

Kiowski, W., 1990. Place of calcium antagonists in the treatment of hypertension. Cor Vasa 32 (2 Suppl. 1), 2–11.

Kruse, A.C., Ring, A.M., Manglik, A., Hu, J., Hu, K., Eitel, K., et al., 2013. Activation and allosteric modulation of a muscarinic acetylcholine receptor. Nature 504, 101–106.

Langmead, C.J., 2011. Determining allosteric modulator mechanism of action: integration of radioligand binding and functional assay data. Methods Mol. Biol. 746, 195–209.

Leppik, R.A., Birdsall, N.J., 2000. Agonist binding and function at the human α_{2A}-adrenoceptor: allosteric modulation by amilorides. Mol. Pharmacol. 58 (5), 1091–1099.

Leppik, R.A., Mynett, A., Lazareno, S., Birdsall, N.J., 2000. Allosteric interactions between the antagonist prazosin and amiloride analogs at the human α_{1A}-adrenergic receptor. Mol. Pharmacol. 57, 436–445.

Lin, R.Z., Chen, J., Hu, Z.W., Hoffman, B.B., 1998. Phosphorylation of the cAMP response element-binding protein and activation of transcription by α_1-adrenergic receptors. J. Biol. Chem. 273 (45), 30033–30038.

Markou, T., Hadzopoulou-Cladaras, M., Lazou, A., 2004. Phenylephrine induces activation of CREB in adult rat cardiac myocytes through MSK1 and PKA signaling pathways. J. Mol. Cell. Cardiol. 37 (5), 1001–1011.

May, L.T., Lin, Y., Sexton, P.M., Christopoulos, A., 2005. Regulation of M2 muscarinic acetylcholine receptor expression and signaling by prolonged exposure to allosteric modulators. J. Pharmacol. Exp. Therapeut. 312 (1), 382–390.

McCune, D., Gaivin, R., Rorabaugh, B., Perez, D., 2004. Bulk is a determinant of oxymetazoline affinity for the α_{1A}-adrenergic receptor. Recept. Channel 10 (3–4), 109–116.

Minneman, K.P., Theroux, T.L., Hollinger, S., Han, C., Esbenshade, T.A., 1994. Selectivity of agonists for cloned α_1-adrenergic receptor subtypes. Mol. Pharmacol. 46 (5), 929–936.

Musselman, D.M., Ford, A.P., Gennevois, D.J., Harbison, M.L., Laurent, A.L., Mokatrin, A.S., et al., 2004. A randomized crossover study to evaluate Ro 115-1240, a selective $\alpha_{1A/1L}$-adrenoceptor partial agonist in women with stress urinary incontinence. BJU Int. 93 (1), 78–83.

O-Uchi, J., Sasaki, H., Morimoto, S., Kusakari, Y., Shinji, H., Obata, T., et al., 2008. Interaction of α_1-adrenoceptor subtypes with different G proteins induces opposite effects on cardiac L-type Ca2+ channel. Circ. Res. 102 (11), 1378–1388.

Ottolini, M., Hong, K., Sonkusare, S.K., 2019. Calcium signals that determine vascular resistance. Wiley Interdiscip. Rev. Syst. Biol. Med. 11 (5), e1448.

Papay, R., Gaivin, R., Archana, J., McCune, D.F., McGrath, J.C., Rodrigo, M.C., et al., 2006. Localization of the mouse α_{1a}-adrenergic receptor in the brain: α_{1a}-AR is expressed in neurons, GABAergic interneurons and NG2 oligodendrocyte progenitors. J. Comp. Neurol. 497, 209–222.

Perez, D.M., DeYoung, M.B., Graham, R.M., 1993. Coupling of expressed α_{1B}- and α_{1D}-adrenergic receptor to multiple signaling pathways is both G protein and cell type specific. Mol. Pharmacol. 44 (4), 784–795.

Perez, D.M., Piascik, M.T., Graham, R.M., 1991. Solution-phase library screening for the identification of rare clones: isolation of an α_{1D}-adrenergic receptor cDNA. Mol. Pharmacol. 40 (6), 876–883.

Perez, D.M., 2020. a1-Adrenergic receptors in neurotransmission, synaptic plasticity, and cognition. Front. Pharmacol. 11, 581098.

Perez, D.M., 2021a. Current developments on the role of α_1-adrenergic receptors in cognition, cardioprotection, and metabolism. Front. Cell Dev. Biol. 9, 652152. https://doi.org/10.3389/fcell.2021.652152.

Perez, D.M., 2021b. Novel positive allosteric modulators of the α_{1a}-adrenergic receptor to treat Alzheimer's disease. Brain Connectivity 11 (1), A10. https://doi.org/10.1089/brain.2020.29017.abstracts. Feb.

Perez, D.M., 2021c. Metabolic therapies for heart failure. Int. J. Mol. Sci. 22 (11), 5783, 2021b.

Perez, D.M., 2007. Structure-function of α_1-adrenergic receptors. Biochem. Pharmacol. 73 (8), 1051–1062.

Rorabaugh, B.R., Ross, S.A., Gaivin, R.J., Papay, R.S., McCune, D.F., Simpson, P.C., Perez, D.M., 2005. The α_{1A}- but not the α_{1B}-adrenergic receptor preconditions the ischemic mouse heart through a staurosporine-sensitive, chelerythrine-insensitive mechanism. Cardiovasc. Res. 65, 436–445.

Scarparo, A.C., Visconti, M.A., Castrucci, A.M., 2006. Signalling pathways evoked by α_1-adrenoceptors in human melanoma cells. Cell Biochem. Funct. 24 (2), 119–129.

Sharpe, I.A., Thomas, L., Loughnan, M., Motin, L., Palant, E., Croker, D.E., et al., 2003. Allosteric α_1-adrenoreceptor antagonism by the conopeptide ρ-TIA. J. Biol. Chem. 278, 34451–34457.

Shi, T., Papay, R.S., Perez, D.M., 2016. α_{1A}-Adrenergic receptor prevents cardiac ischemic damage through PKCδ/GLUT1/4-mediated glucose uptake. J. Recept. Signal Transduction 36 (3), 261–270.

Sinner, B., Steiner, J., Malsy, M., Graf, B.M., Bundscherer, A., 2019. The positive allosteric modulation of $GABA_A$ receptors mRNA in immature hippocampal rat neurons by midazolam affects receptor expression and induces apoptosis. Int. J. Neurosci. 129 (10), 986–994.

Sugimoto, T., Morioka, N., Sato, K., Hisaoka, K., Nakata, Y., 2011. Noradrenergic regulation of period1 expression in spinal astrocytes is involved in protein kinase A, c-Jun N-terminal kinase and extracellular signal-regulated kinase activation mediated by α_1- and β_2-adrenoceptors. Neuroscience 185, 1–13.

Szlenk, C.T., Gc, J.B., Natesan, S., 2021. Membrane-facilitated receptor access and binding mechanisms of long-acting β2-adrenergic receptor agonists. Mol. Pharmacol. 100 (4), 406–427.

Targowska-Duda, K.M., Kaczor, A.A., Jozwiak, K., Arias, H.R., 2018. Molecular interactions of type I and type II positive allosteric modulators with the human α7 nicotinic acetylcholine receptor: an *in silico* study. J. Biomol. Struct. Dyn. 16, 1–29.

Thonberg, H., Fredriksson, J.M., Nedergaard, J., Cannon, B., 2002. A novel pathway for adrenergic stimulation of cAMP-response-element-binding protein (CREB) phosphorylation: mediation via α_1-adrenoceptors and protein kinase C activation. Biochem. J. 364 (Pt 1), 73–79.

Valant, C., Felder, C.C., Sexton, P.M., Christopoulos, A., 2012. Probe dependence in the allosteric modulation of a G protein-coupled receptor: implications for detection and validation of allosteric ligand effects. Mol. Pharmacol. 81, 41–52.

Waugh, D.J., Gaivin, R.J., Zuscik, M.J., Gonzalez-Cabrera, P., Ross, S.A., Yun, J., Perez, D.M., 2001. Phe-308 and Phe-312 in transmembrane domain 7 are major sites of α_1-adrenergic receptor antagonist binding. Imidazoline agonists bind like antagonists. J. Biol. Chem. 276 (27), 25366–25371.

Waugh, D.J., Zhao, M.M., Zuscik, M.J., Perez, D.M., 2000. Novel aromatic residues in transmembrane domains IV and V involved in agonist binding at a1A-adrenergic receptors. J. Biol. Chem. 275 (16), 11698–11705.
Whitlock, G.A., Conlon, K., McMurray, G., Roberts, L.R., Stobie, A., Thurlow, R.J., 2008. Novel 2-imidazoles as potent and selective alpha1A adrenoceptor partial agonists. Bioorg. Med. Chem. Lett 18 (9), 2930–2934.
Wold, E.A., Chen, J., Cunningham, K.A., Zhou, J., 2019. Allosteric modulation of class A GPCRs: targets, agents, and emerging concepts. J. Med. Chem. 62 (1), 88–127.
Wootten, D., Christopoulos, A., Sexton, P.M., 2013. Emerging paradigms in GPCR allostery: implications for drug discovery. Nat. Rev. Drug Discov. 12 (8), 630–644.